



Synthesis and Biological Evaluation of Novel Thiazole Derivatives as Anti-Diabetic Potential Agents



Fawziah A. Al-Salmi

Department of Biology, College of Science, Taif University, P.O. Box 11099, Taif 21944, Saudi Arabia

Abstract

Diabetes mellitus is considered as a chronic disease causing oxidative stress that promotes tissue damage. The purpose of this work is to evaluate the antioxidant activity of new hydrazine thiazole derivatives *in vitro*. Considering the diverse array of biological activities exhibited by thiazole derivatives. A new series of hydrazine thiazole was prepared following the Hantzsch method. Physical characteristics (melting point) were used to initially validate each compound. Afterwards, a variety of spectroscopic methods, including ¹H, ¹³C-NMR, and mass spectrometry, confirmed these results. All components' binding interactions were investigated through the use of a molecular docking simulation technique. Additionally, the potential of each component in terms of α -glucosidase and antioxidants was assessed. All synthesized derivatives were approved biocompatible with blood glucose levels in diabetics compared to the standard acarbose. Among the examined components, compared to acarbose (IC₅₀ = 0.597 ± 0.022 μ M), analogue (3) (IC₅₀ = 0.69 ± 0.025 μ M) was discovered to be a highly potent contender against α -glucosidase. Docking studies further supported the antidiabetic potential. All of the synthesized components showed a variety of interactions along the active sites of the enzymes with varying binding energies, according to docking experiments.

Keywords: α -Glucosidase inhibitory, DPPH radical scavenging, Diabetes mellitus, acarbose, COX-1inhibitory

1. Introduction

Thiazoles are organic five aromatic ring structures. Hantzsch and Weber originally reported the powerful biological effects of thiazoles in 1887 [1-3]. One of the most valuable structural moieties in modern medicinal chemistry is a thiazolone template because of its broad pharmacological spectrum and affinities for the biotargets of different heterocyclic compounds [4-8]. A few thiazolidinones showing hypoglycemia, antineoplastic, and anti-inflammatory activities [9-12]. The human body produces reactive species as a result of regular biochemical processes, which the body's antioxidant defense system can effectively combat. However, an imbalance can result from either an increase in these interactive types production or a decrease in the body's defenses. In these situations, interactive types cause cumulative damage to biomolecules like amino acids, lipids, and DNA, and they are linked to several chronic diseases, including diabetes mellitus. Oxidative stress is the term for this state [13-17]. We attempt to investigate in this work how the thiazolone scaffold mixture and the pyrazoline moiety affect the anti-diabetic activity. Diabetes mellitus is a chronic systemic disease defined by abnormally increased levels of glucose in blood due to the inability of the body to utilize insulin. It was recently demonstrated that these new thiazolone derivatives as bioactive arms on heterocyclic scaffolds that are beneficial for the pharmacological effect implementation of drugs based on thiazolones. There is a vast demand of the structurally complex thiazolone scaffolds. Synthesized compounds (3 and 7) have been shown most promising antidiabetic activity.

2. Materials & methods

General

Using a Perkin Elmer Avator series FT-IR spectrophotometer, the IR-spectra of a few produced 2,4-disubstituted-1,3-thiazoles were recorded as KBr-max. A Perkin-Elmer CHN-elemental is used for the micro analysis. The electro thermal 9200 numerical m.p. system is used to calculate the melting point, and it was left uncorrected. The molecular weight of the same prepared compounds is proven using an electron ionization mass spectrometer ("EI-MS") on a robe "Agilent MSD-5978 spectrometer" with 70 eV. ¹H and ¹³C NMR ranges in the specified solvents are measured on a DPX-400 spectrometer (Bruker). All components are of the analytical degree, and kits that are available commercially that is gained from either Aldrich or Sigma and all chemicals are of analytical degree.

Syntheses of 2,4-dihydroxyacetophenone thiosemicarbazone (2).

A mixture of 2,4-di-OH-acetophenone (1.52 g, 0.01 mole), and thiosemicarbazide (0.91 g, 0.01 mole) in 30 mL ethanol with AcOH, were heated for 4 hrs, then slowly cooled to 25 °C. The formed solid is separated by filtration, washed with EtOH, dried, and crystallized with EtOH to produce (2) as brown crystals; yield 86%; mp 178-180 °C; ¹H-NMR (400 MHz, DMSO-*d*₆): δ 2.36 (s, 3H, CH₃), 6.21 (s, 1H, H-Aromatic), 7.38-7.92 (m, 4H, H-Aromatic, and NH₂), 10.01 (br.s, 1H, OH), 11.35 (s, 1H, NH),

*Corresponding author e-mail: fawziahaalsalmi@gmail.com; f.alsalmi@tu.edu.sa; (Fawziah A. Al-Salmi).

Received Date: 10 September 2024, Revised Date: 10 November 2024, accepted Date: 23 November 2024

DOI: <https://doi.org/10.21608/ejchem.2024.319761.10392>

©2025 National Information and Documentation Center (NIDOC)

12.31 (s, 1H, OH) ppm; CHN analysis calcd for C₉H₁₁N₃O₂S [225]: C, 47.99; H, 4.92; N, 18.65. Found: C, 47.88; H, 4.56; N, 18.33.

Synthesis of 2-(2,4-dihydroxyphenylethylidene)-hydrazino-1,3-thiazol-4-(5H)-one (3) A solution of thiosemicarbazone derivative (**2**, 2.25 g, 0.01 mole), and anhydrous K₂CO₃ (1.38 gm, 0.01 mole) in (70 mL) EtOH was refluxed for 30 min., ethyl chloroacetate (1.22 mL, 0.01 mole) was added. Then reaction was refluxed for 3 hrs, then cooled at 25 °C, and poured into H₂O, and neutralized with diluted HCl (2N) with stirring, the solid obtained was filtered off, washed with H₂O and dried. lastly, the result was recrystallized from EtOH to afford (**3**) as orange crystals, yield; 78%; mp 251-253 °C; IR: (KBr, cm⁻¹) 3449, 3380 (br. OH), 3221 (NH), 1689 (C=O), 1633 (C=N), 1605, 1583 (C=C), 1098, 1033 (C-O); ¹H NMR (400 MHz, DMSO-*d*₆): δ 2.42 (s, 3H, CH₃), 3.89 (s, 2H, CH₂ of thiazole ring), 6.30 (s, 1H, H- Aromatic), 6.36-6.38 (d, 1H, J = 8.8 Hz, H- Aromatic), 7.42-7.45 (d, 1H, J = 8.8 Hz, H- Aromatic), 10.01 (br.s, 1H, OH), 11.38 (br.s, 1H, NH), 12.95 (br.s, 1H, OH) ppm; ¹³C NMR (DMSO-*d*₆, 100 MHz): δ 176.55 (C-2 of thiazole), 164.96 (C=O), 164.87 (C=N), 161.57, 161.09 (2x C-O), 130.69, 111.95, 107.71, 103.33 (C-aromatic), 34.62 (CH₂ of thiazole), 14.54 (CH₃) ppm; CHN analysis calcd for C₁₁H₁₁N₃O₃S [265]: C, 49.80; H, 4.18; N, 15.84. Found: C, 49.63; H, 4.03; N, 15.58.

General procedure for the synthesis of (5 and 6) A mixture of (**3**) (2.65 g, 0.01 mole), methyl acrylate (0.86 g, 0.01 mole) and/or ethyl chloroacetate (1.22 g, 0.01 mole) in 50 mL EtOH in the presence of Et₃N (2 mL) was heated for 7 hrs. additional the reaction was cooled at 25 °C, poured into H₂O, and neutralized with HCl_{dil} (2N). Following clarification, the product was collected, washed with H₂O, dried, and finally crystallized from ethanol to give (**5**) and (**6**).

Methyl-[2-(2,4-hydroxyphenylethylidene)-1-(4-oxo-5-hydro-1,3-thiazol-2-yl) hydrazine]propionate (5) was obtained as yellow crystals; yield 73%; mp 220-222 °C; IR: (KBr, cm⁻¹) 3455, 3389 (br.OH), 1753, 1693 (C=O), 1630 (C=N), 1605, 1588 (C=C), 1120, 1098, 1021 (C-O); ¹H NMR (400 MHz, DMSO-*d*₆): δ 2.37, 2.42 (s, 3H, CH₃ of two isomer), 2.95 (t, 2H, COCH₂), 3.53 (t, 2H, NCH₂), 3.86 (s, 3H, OCH₃), 4.06 (s, 2H, CH₂ of thiazole ring), 6.32 (br.s, 1H, H- Aromatic), 6.38 (br.d, 1H, H- Aromatic), 7.43 (d, 1H, H- Aromatic), 10.06 (s, 1H, OH), 12.71 (br.s, 1H, OH) ppm; ¹³C NMR (DMSO-*d*₆, 100 MHz): δ 171.98, 171.95 (C-2 of thiazole of two isomer), 167.94 (C=O of ester), 161.64, 161.59 (C=O), 161.41 (C=N), 160.19, 159.75 (C-O), 131.15, 118.94, 111.81, 108.09, 103.35 (C-aromatic), 52.16 (CH₃), 45.58 (NCH₂), 33.15, 31.52 (CH₂ of thiazole ring of two isomer), 15.74 (CH₂CO), 14.71, 14.56 (CH₃ of two isomer) ppm; CHN analysis calcd for C₁₅H₁₇N₃O₅S [351]: C, 51.27; H, 4.88; N, 11.96. Found: C, 51.03; H, 4.58; N, 11.66.

Ethyl-[2-(2,4-dihydroxyphenylethylidene)-1-(4-oxo-5-hydro-1,3-thiazol-2-yl) hydrazino]acetate (6) was obtained as yellow crystals; yield 69%; mp 224-226 °C; IR: (KBr, cm⁻¹) 3433, 3365 (br.OH), 1776, 1693 (C=O), 1629 (C=N), 1603, 1582 (C=C), 1121, 1098, 1022 (C-O); ¹H NMR (400 MHz, DMSO-*d*₆): δ 1.20-1.24 (t, 3H, J = 7.2 Hz, CH₃), 2.42 (s, 3H, CH₃), 4.16-4.22 (m, 4H, OCH₂ and CH₂ of thiazole ring), 4.53 (s, 2H, NCH₂CO), 6.29 (s, 1H, H- Aromatic), 6.36-6.39 (dd, 1H, J = 8.8 and J = 2.00 Hz, H- Aromatic), 7.48-7.51 (d, 1H, J = 8.8, H- Aromatic), 10.07 (s, 1H, OH), 12.72 (s, 1H, OH) ppm; ¹³C NMR (DMSO-*d*₆, 100 MHz): δ 171.76 (C-2 of thiazole), 167.88, 167.41 (C=O), 161.79, 161.58, 159.67 (C-O and C=N), 131.29, 111.57, 107.94, 103.31 (C-aromatic), 61.76 (OCH₂), 14.54, 14.48 (2CH₃) ppm; CHN analysis calcd for C₁₅H₁₇N₃O₅S [351]: C, 51.27; H, 4.88; N, 11.96. Found: C, 51.05; H, 4.52; N, 11.59.

General procedure for the synthesis of (4 and 7) A solution of compounds **3** and/or **6** (2.65 g, 3.51 gm, 0.01 mole) in Ac₂O (30 mL) was reflux-warmed for 2h, then child along emptied into ice-H₂O. The reaction amalgam was dropped for one day, and the precipitate created was sorted off, washed with H₂O, and dry, Lastly, the result was recrystallized from EtOH to give (**4** and **7**).

2-[(2-Acetoxy-4-hydroxyphenylethylidene)-1-acetoxyhydrazino]- 1,3-thiazol-4-(5H)-one (4) was obtained as colorless crystals; yield 61%; mp 203-205 °C; IR: (KBr, cm⁻¹) 3433 (br.OH), 1775, 1760, 1693 (C=O), 1632 (C=N), 1610, 1591 (C=C), 1187, 1083, 1031 (C-O); ¹H NMR (400 MHz, DMSO-*d*₆): δ 1.93, 1.95 (s, 3H, COCH₃ of two isomer), 2.17, 2.18 (s, 3H, COCH₃ of two isomer), 2.23, 2.31 (s, 3H, CH₃ of two isomer), 3.73, 3.87 (s, 2H, CH₂ of thiazole of two isomer), 6.72 (s, 1H, H- Aromatic), 6.73-7.79 (m, 1H, H- Aromatic), 12.15 (br.s, 1H, OH), 12.89 (s, 1H, OH) ppm; ¹³C NMR (DMSO-*d*₆, 100 MHz): δ 174.09 (C-2 of thiazole), 165.93 (164.52), 163.73 (163.01) (C=O), 160.55, 153.28, 151.62 (C-O and C=N), 149.26 (148.74), 130.62 (130.55), 127.24, 120.04, 118.28, 117.81 (117.50), 113.17, 112.82, 110.69, 80.19 (79.99) (C-aromatic), 34.03 (CH₂ of thiazole ring), 22.23, 22.11, 21.47, 21.39, 21.29, 21.17 (COCH₃ of two isomer), 18.29, 14.94 (CH₃ of two isomer) ppm; CHN analysis calcd for C₁₅H₁₅N₃O₅S [349]: C, 51.57; H, 4.33; N, 12.03. Found: C, 51.33; H, 4.11; N, 11.97.

Ethyl-[2-(2-acetoxy-4-hydroxyphenylethylidene)-1-(4-oxo-5-hydro-1,3-thiazol-2-yl)-1-acetylhydrazino]-acetate (7) was obtained as colorless crystals; yield 64%; mp 179-181 °C; IR: (KBr, cm⁻¹) 3432 (br.OH), 1756, 1705, 1689 (C=O), 1628 (C=N), 1610, 1591 (C=C), 1125, 1099, 1022 (C-O); ¹H NMR (400 MHz, DMSO-*d*₆): δ 1.20-1.23 (t, 3H, J = 7.20 Hz, CH₃), 1.70 (s, 3H, COCH₃), 2.28, 2.41 (s, 3H, CH₃), 4.15-4.24 (m, 4H, OCH₂ and CH₂ of thiazole ring), 4.52 (s, 2H, NCH₂CO), 6.27 (s, 1H, H- Aromatic), 6.35-6.73 (d, 1H, J = 8.40 Hz, H- Aromatic), 7.42-7.44 (d, 1H, J = 8.80 Hz, H- Aromatic), 12.66 (br.s, 1H, OH) ppm; ¹³C NMR (DMSO-*d*₆, 100 MHz): δ 175.38, 171.82, 171.75 (C-2 of thiazole of two isomer), 169.31, 168.90, 167.91, 167.71, 167.61, 167.41, 167.36, 163.37 (C=O), 161.87, 161.51, 160.64, 159.10, 153.49 (C-O and C=N), 131.03, 130.82, 113.15, 110.73, 110.62, 108.59, 106.96, 103.51 (C-aromatic), 61.75 (OCH₂), 44.22 (NCH₂CO), 33.15, 31.16 (CH₂ of thiazole ring of two

isomer), 25.04, 21.37 (OCOCH₃ of two isomer), 14.97, 14.53 (2CH₃) ppm; CHN analysis calcd for C₁₇H₁₉N₃O₆S [393]: C, 51.90; H, 4.87; N, 10.68. Found: C, 51.72; H, 4.63; N, 10.24.

Biological methods

α -glucosidase inhibitory assay

A 95-well plate was pre-incubated at 36°C for 20 mins with a reaction mixture that included 40 μ l of phosphate buffer (40 mM, pH = 6.7), 15 μ l of α -glucosidase from *Saccharomyces cerevisiae* (1U/ml) (#G5003, Sigma), and 25 μ l of several doses of the produced components. Following that, 25 μ l of *p*-NO₂-phenyl-D-glucopyranoside (2 mM) [SRL] (#487506, Sigma) was added as a substrate, and the mixture was incubated for 25 mins at 37°C. The injection of 40 μ l Na₂CO₃ (0.01M) stopped the process. At 400 nm, the produced color was measured with a Multimode Reader (Synergy HT, BioTek). Every experiment was run three times, with enough blanks in between. Different acarbose concentrations were employed as a control. Negative control was set up concurrently. The result is shown as an inhibition percentage (%), which was computed using the formula Inhibition (%) = $\frac{A_{\text{Negative control}} - A_{\text{Test}}}{A_{\text{Negative control}}} \times 100$, where A stands for absorbance. An IC₅₀ value is another way to convey the outcome [28].

DPP-IV inhibitory activity assay

An investigation was conducted on the in vitro DPP-4 (human recombinant enzyme) inhibition of the synthetic (**4**) using the Fluorogenic DPP4 Assay Kit (BPS Bioscience, Catalogue #: 80204). The Fluorogenic DPP4 Assay Kit uses purified DPP4 to measure DPP4 activity for screening and profiling. It comes with pure DPP4 enzyme, DPP substrate, and DPP assay buffer in a small 95-well configuration with 99 enzyme reactions. The Fluorogenic DPP4 Assay Kit's unique fluorogenic substrate is its trade secret. This kit only needs one simple step on a microliter plate for DPP4 responses. A fluorescence reader is used to quantify the fluorophore produced by incubating a sample containing the DPP4 enzyme with the fluorometric substrate. The results were represented by IC₅₀ values, which were computed [29-31].

DPPH scavenging assay

Free radical scavenging efficacy of the produced components was assessed by 1,1-di-ph-2-picryl hydrazyl. To put it briefly, ethanol was utilized to create a 0.01 mM DPPH solution. This solution was added to 2 mL of several extracts in EtOH. In this case, dilution is used to create a range of quantities of synthetic compounds that have been dissolved in dimethyl sulfoxide. After giving the mixture a good shake, it was allowed to stand at 25°C for 25 mins. After then, absorbance at 510 nm was measured using a spectrophotometer. The experiment was run in triplicate by ascorbic acid as the reference standard component. The sample's IC₅₀ value, or the concentration of sample needed to inhibit 50% of the DPPH free radical, was found using the Log Doseage Inhibition Curve. Reduced absorbance in the reaction indicated increased free radical activity. The DPPH scavenging effect was calculated by this equation: $\frac{A_0 - A_1}{A_0} \times 100$ is the percent inhibition or DPPH scavenging action (%). The absorbance of the standard sample was denoted by A₁, and the absorbance of the control reaction was denoted by A₀ [32,33].

COX-1 inhibitory activity assay

Using an in vitro enzymatic assay, the compounds' inhibitory activity was examined. 170 μ L of 101 mM Tris buffer (pH = 7.9), which contained 17 mM L-epinephrine, 5.00 μ M porcine hematin, and 55 μ M Na₂EDTA, was mixed with 1 unit/reaction of ovine COX-1. To the reaction was added 10 μ L of the tested chemical dissolved in dimethyl sulfoxide (as a blank). The reference inhibitors were (S)-(+)-Ibuprofen and the selective COX-1 inhibitor SC-560 (both from Sigma-Aldrich, USA). Reaction was started with 6 μ L of arachidonic acid (11 μ M) and incubated for 25 minutes at 36°C after 6 minutes at 25°C. Next, 25 μ L of HCOOH (15% v/v) was added to halt the reaction. Using an ELISA kit (Enzo Life Sciences, USA), the concentration of prostaglandin E₂ (PGE₂) was determined. The mixture was diluted 1:10 in the kit's assay buffer, and it was then incubated in accordance with the manufacturer's recommendations. Using an Infinite M200 microplate reader (Tecan Group, Switzerland) to measure absorbance at 410 nm, the concentration of PGE₂ produced during the reaction was determined. In comparison to a blank, the percentual inhibition of PGE₂ production was used to calculate the inhibitory activity. Initially, the compounds' inhibitory action was measured at 25 μ M to determine if any activity was present. Only substances that inhibited COX-1 to at least 90% had IC₅₀ values calculated. Based on the percentual inhibition induced by the reference chemical ibuprofen, the percentual inhibition level was selected. Every experiment was conducted in triplicate and at least twice over. to investigate the possibility that a higher substrate concentration affects a compound's activity [34].

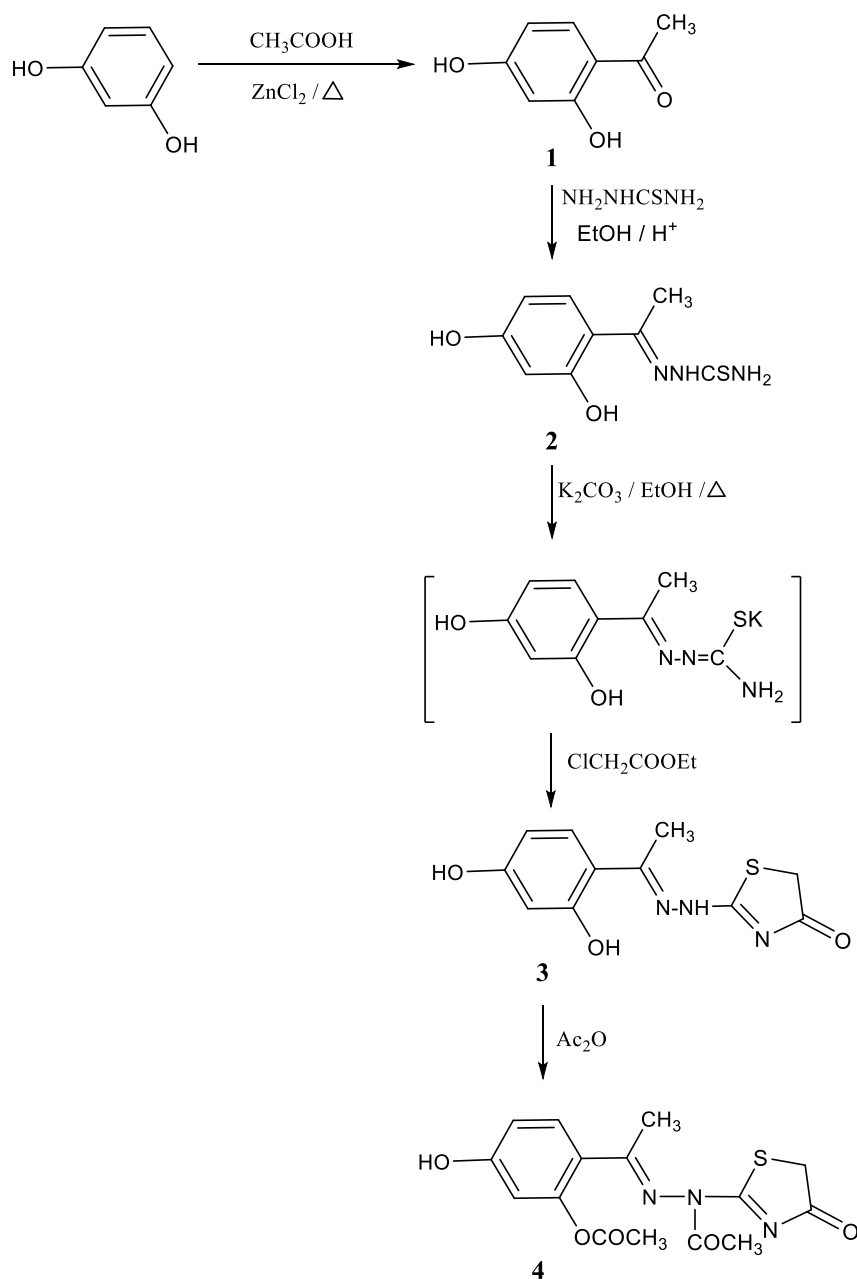
Molecular Docking

Acarbose (PDB: 5NN8) forms a complex with human lysosomal α -glucosidase [35]. The α -glucosidase protein receptor's 3D X-ray crystal structure was retrieved from the Protein Data Bank (<https://www.rcsb.org/>). The receptor protein underwent three-dimensional protonation, hydrogen addition, energy minimization, and ligand active site prediction in order to get ready for molecular docking. Subsequently, MOE software was used to dock compounds with the target protein (α -glucosidase) using the Triangle Matcher placement approach. In order to see the ligand-protein interaction during docking, the ligand was chosen, and rescoring was set at London dG and rescoring at GBVI/WSA dG, running. The 2D and 3D structures, ligand characteristics, and protein-ligand docking score were preserved [36-39].

3. Result and discussion

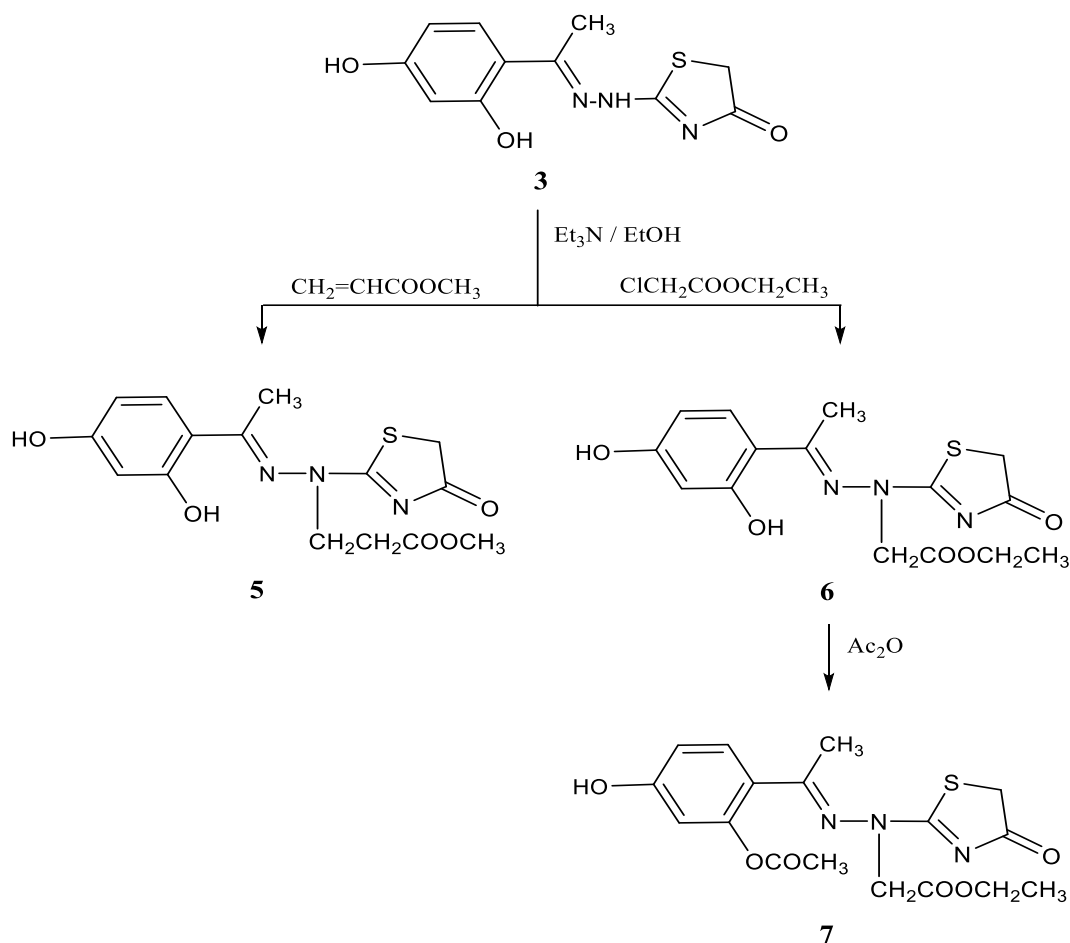
The synthesis of target components 2-substituted-1,3-thiazol-4(5H)-one were achieved by synthetic route in scheme 1 and 2. The reaction of resorcinol with AcOH/EtOH under heating lead to the formation of 2,4-di-OH-acetophenone (**1**) [18,19], followed by the condensation of (**1**) with thiosemicarbazide in ethanol/H⁺ catalyst prior to the formation of key substrate 2,4-

dihydroxyacetophenone thiosemicarbazone (2) [20]. Treatment of carbazone (2) with ethyl chloroacetate in anhydrous K_2CO_3 under heat to give the 2-(2,4-dihydroxy phenyl ethylidene)hydrazine-1,3-thiazol-4(5H)-one (3). Compound (3) was confirmed via its transformation into 2-(4-hydroxy-2-acetoxyphenylethylidene)acetylhydrazino-1,3-thiazol-4-(5H)-one (4) via acetylation of 2-(2,4-dihydroxyphenylethylidene)hydrazine-1,3-thiazol-4-(5H)-one (3) with acetic anhydride under reflux [21].



Scheme 1: Synthesis of 2-(2,4-dihydroxyphenylethylidene)-1,3-thiazol-4-(5H)-one and their acetyl derivative (**4**)

Additionally, reaction of 2-(2,4-dihydroxyphenylethylidene)hydrazine-1,3-thiazole-4-(5H)-one (**3**) with methyl acrylate and ethyl chloroacetate in EtOH in the presence triethyl amine as base catalyst yielded the corresponding methyl[1-(thiazole-4-(5H)-one-2-yl)-2-(2,4-dihydroxyphenylethylidene)hydrazine]-propionate (**5**) and ethyl[1-(4-oxo-5-hydrothiazol-2-yl)-2-(2,4-dihydroxyphenylethylidene)hydrazine]acetate (**6**), respectively. Acetylation of (**6**) with Ac_2O under boiling afforded [1-(4-oxo-5-hydrothiazole-2-yl)-2-(2-acetoxy-4-hydroxyphenylethylidene)hydrazino]-acetate (**7**).



Scheme 2: Synthesis of 2-substituted-1,3-thiazol-4-(5H)-one derivatives (5-7)

NMR spectra investigation of synthesized 2-substituted-1,3-thiazol-4-(5H)-one derivatives (3-7)

In order to elucidate structural features of the compounds, ^1H , and ^{13}C -NMR spectra of the 2-substituted-1,3-thiazolone derivatives were investigated. From the data of ^1H -NMR spectrum (**Figure S1a**) for the compound (**3**) gave clear evidence two signals of singlet at δ 2.41 and 3.89 ppm for the CH_3 protons of ethylidene group and methylene protons (SCH_2CO) of thiazole ring. The aromatic protons of 2,4-dihydroxyphenyl appeared in the ^1H -NMR as singlet signal at δ 6.30, a double doublet signal at δ 7.42-7.45 of each three protons of Ar-H, while the proton of hydroxyl group of 3,4-hydroxy appeared at δ 9.98, 12.95 ppm and NH at δ 4.38 ppm. The ^{13}C -NMR of compound (**3**) revealed a characteristic carbon signals at δ 176.36 (C-2 of thiazole ring), 164.96 (C=O of thiazole ring), 164.87 (C=N), and 161.57, 161.09 (two C-O) ppm. The four carbon signals of aromatic ring are observed at δ 130.69, 111.95, 107.71, and 103.33 ppm, while the carbon signal of CH_2 of thiazole ring and carbon signal of CH_3 proton appeared at δ 34.62 and 14.54 ppm, respectively (**Figure S1b**). The ^1H -NMR spectra of (**5 and 6**) presented new protons signals at δ 2.95, 3.53, and 3.86 due to the $-\text{CH}_2\text{CH}_2\text{COOCH}_3$ group of (**5**), while the new proton signals of compound (**6**) at δ 1.22 (t), 4.18 (q), and 4.53 (s) due to the $-\text{CH}_2\text{COOCH}_2\text{CH}_3$ groups with absence the proton signal of NH group for the compound (**3**) at δ 11.35 ppm. The proton signals of CH_3 , CH_2 of thiazole ring, and Ar-proton ring ($\text{CH}=\text{CH}$) detected at δ 2.34-2.43 of CH_3 as singlet signal, 4.01-4.13 as singlet signal of methylene protons of thiazole ring, at δ 6.29 as singlet of one proton, at 6.36-6.39 as double doublet of one proton of aromatic, and at δ 7.48-7.51 ppm as doublet signal for one proton of aromatic ring. The ^{13}C -NMR spectra of (**5 and 6**) exhibited two singles signals at δ 31.52, 33.15 ppm of compound (**5**), while at δ 31.15, 33.07 ppm due to the carbon of methylene group in thiazole ring showed the structures of (**5 and 6**) in two isomers (cis & trans isomers) as shown in (**Figure 1**).

effectiveness in managing postprandial blood glucose levels in diabetics [23]. The findings demonstrated that the substances had a significant inhibitory effect on the activity of α -glucosidase, as depicted in (Figure 3). Table 1 presents a summary of the coumarins' enzyme inhibiting actions. Compared to standard acarbose ($IC_{50} = 0.59 \mu\text{g/ml}$), the synthesized components demonstrated strong inhibitory effects against α -glucosidase, with IC_{50} values ranging from 0.69 to 2.45 $\mu\text{g/ml}$. Furthermore, compound (3) showed encouraging α -glucosidase inhibition, with an IC_{50} equal 0.69 $\mu\text{g/ml}$.

Table 1: The produced compounds inhibitory effects on the activity of the α -glucosidase enzyme.

Compounds	α -glucosidase inhibitory assay	
	IC_{50} ($\mu\text{g/ml}$) ^a	
3	0.69±0.025	
4	1.08±0.04	
5	1.13±0.042	
6	2.45±0.09	
7	0.86±0.031	
Acarbose ^b	0.597±0.022	

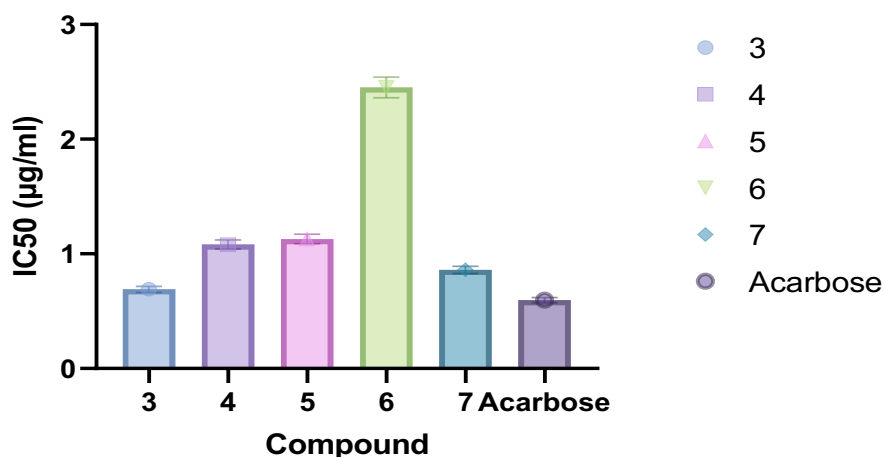


Figure 3: α -glucosidase IC_{50} values of the synthesized components are shown graphically.

DPP-4 inhibitory activity

Subsequently, we examined the synthetic drugs' inhibition of DPP-4 activity to further understand their antidiabetic characteristics. While DPP-4 is essential for glucose and insulin metabolism, its precise functions remain unclear. DPP-4 degrades incretins such as GIP and GLP-1, resulting in aberrant visceral adipose tissue metabolism and decreased insulin production. Conversely, by degrading GLP-1, DPP-4 allows for the regulation of postprandial glucose [24]. The synthetic component (3) was assessed for its in vitro DPP-4 inhibitory efficiency, as depicted in Figure 4. The inhibition activity of the component at different concentrations are listed in Table 2. Results showed that component (3) had excellent inhibitory activity at 100 $\mu\text{g/ml}$. Compound (3) showed good DPP-4 inhibitory activity with an IC_{50} equal 0.304 $\mu\text{g/ml}$, compared to sitagliptin with IC_{50} equal 0.068 $\mu\text{g/ml}$.

Table 2: Component (3)'s in vitro DPP-4 inhibitory action

Compound	Concentration ($\mu\text{g/ml}$) and inhibition %					IC_{50} ($\mu\text{g/ml}$)
	0.01	0.1	1	10	100	
3	25.5	37.4	59.9	80.9	92.4	0.304±0.012
Sitagliptin	31.7	56.3	72.2	86.5	95.9	0.068±0.003

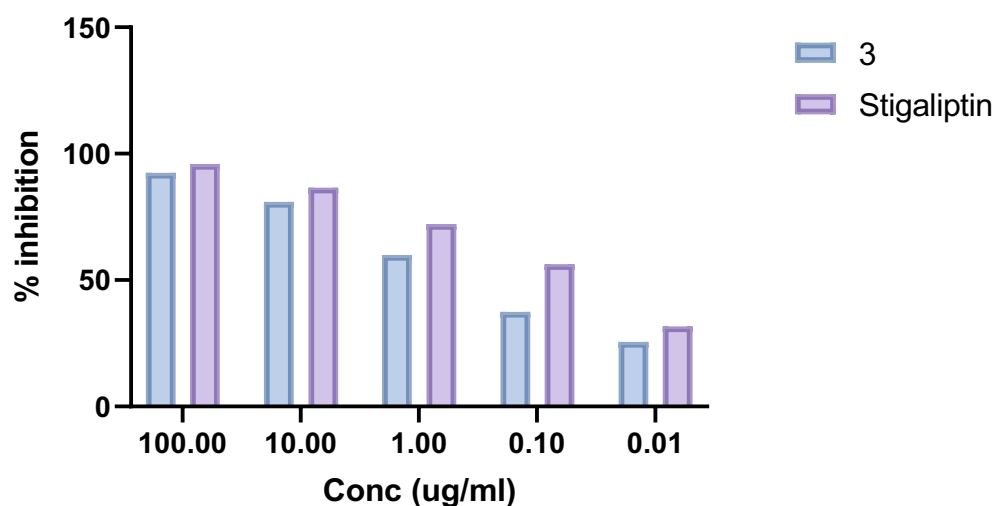


Figure 4: Compound 3's DPP-4 inhibitory activity at different doses is shown graphically.

DPPH radical scavenging assay

The ability of synthetic component (**3**) to scavenge the DPPH radical was investigated using quercetin as the reference medication. As **Table 3** illustrates, we investigated the impact of the synthesized compound's inhibitory activity at different doses. Compared to quercetin ($IC_{50} = 12.11 \pm 0.49$ ug/ml), the synthesized drug had superior radical scavenging ability, as demonstrated by its IC_{50} value of 34.54 ± 1.4 ug/ml (**Figure 5**).

Table 3: In vitro DPPH scavenging activity of compound (3).

Compound	Concentration (ug/ml) and inhibition %					IC_{50} (ug/ml)
	10	25	75	150	300	
3	25	47	66	76	88	34.54 ± 1.4
Quercetin	47	60	73	82	90	12.11 ± 0.49

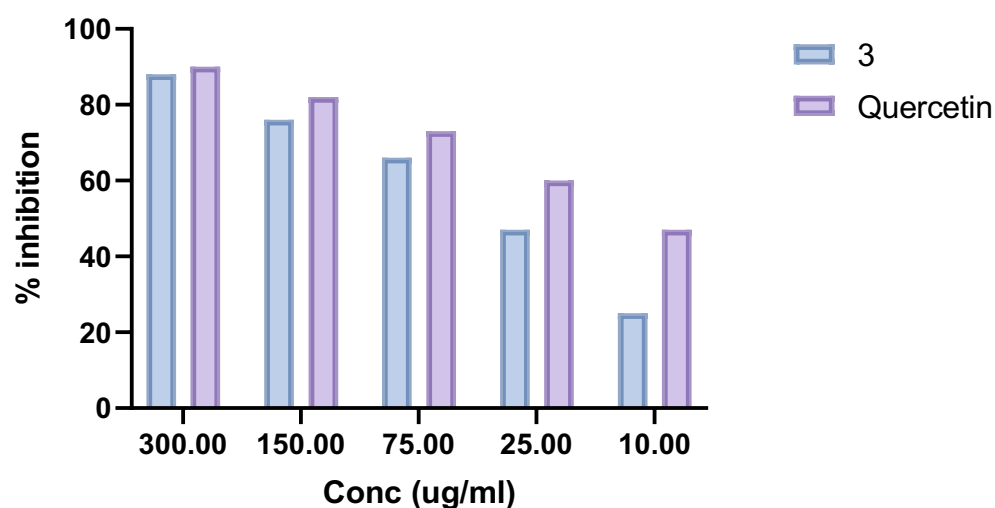


Figure 5: Compound 3's DPPH inhibitory action at different doses is shown graphically.

COX-1inhibitory activity

The enzyme cyclooxygenase-1 performs a key role in the production of prostaglandins, which are lipid compounds that perform various physiological functions, including the regulation of inflammation, maintenance of the stomach lining, and support of platelet function. COX-1 is constitutively expressed in most tissues, meaning it is produced at constant levels and is involved in the normal physiological maintenance of tissues. Understanding COX-1's functions and its inhibition is crucial for the development of drugs with fewer side effects [24]. Compound 3 showed excellent COX-1inhibitory activity with an IC₅₀ equal 6.77±0.25 ug/ml, compared to Ibuprofen with an IC₅₀ equal 2.18±0.08 ug/ml.

Molecular docking study

In order to gain additional knowledge on the kinds of binding interactions and the residues of amino acids that initiate the biological activities of (**3 and 7**), there were investigations done with molecular docking. Docking simulation analysis was carried out between compounds (**3 and 7**) in this research work and the α -glucosidase protein receptor's binding site and evaluated to determine the affinity scores and mode of interaction (hydrophobic and hydrophilic) and the results are showed in **Table 4**. The alpha-glucosidase receptor's binding sites are seen to have been impacted by compounds (**3 and 7**). 2D & 3D binding nature of compounds (**3 and 7**) in the binding pockets of the alpha-glucosidase receptor were shown in **Figures 6-8**. Having high blood sugar is a sign of type 2 diabetes, which alters how the body consumes and metabolizes sugar [25]. People who have this long-term illness run a significant risk of developing cardiovascular disease, nephritis, blindness, and dying young. Positive dietary modifications can be made by people with type 2 diabetes. Glucose polymers, which are frequently present in breads, potatoes, and cereal grains, make up dietary carbs and starches. Alpha-glucosidase is an enzyme that breaks down glucose polymers into monosaccharides. Consuming too much of these can cause insulin resistance, which is strongly linked to diabetes. Diabetes can be treated by inhibiting α -glucosidase, which directly suppresses the breakdown of carbohydrates. Alpha-glucosidase inhibitors, such as voglibose, miglitol, and acarbose, have been used to treat type 2 diabetes up till now. They can effectively delay the intestinal absorption of carbohydrates, hence lowering postprandial blood glucose levels [25]. However, these medications' adverse effects significantly limit their uses [26,27].

Table 4: Interactions data comparison of compounds (3 and 7) with active site of α -glucosidase receptor.

Compound	Receptor (PDB)	S (kcal/mol)	RMSD (Å)	Hydrophilic Interactions	Hydrophobic Interactions
Compound 3	5NN8	-5.05	2	Asp518 Asp404 Asp616	Ile441, Phe649, Trp516, Met519, Trp376, Leu405, Trp481
Compound 7		-6.4	1.3	Asp616 Arg600 Asp282	Phe525, Phe649, Trp516, Met519, Trp376, Trp613, Leu650, Leu677, Leu678, Trp481
Acarbose		-7.95	0.4	Asp404 His674 Asp518 Asp616 Arg600 Met519 Asp282	Phe649, Trp613, Trp481, Ile441, Leu405, Trp376, Trp516

The results revealed that the NH group and S-atom of compound (**3**) bound through hydrogen bonds to protein residue (Asp616). In addition, protein residues (Asp518 and Asp404) bound through hydrogen bonds to component (**3**). Furthermore, the S-atom of (**7**) bound through hydrogen bonds to protein residues (Asp616, Arg600, and Asp282). Moreover, the phenolic (OH) groups and NH₂⁺ of reference drug (acarbose) bound through hydrogen bonds to protein residues (Asp404, His674, Asp518, Asp616, Arg600, Met519, Asp282).

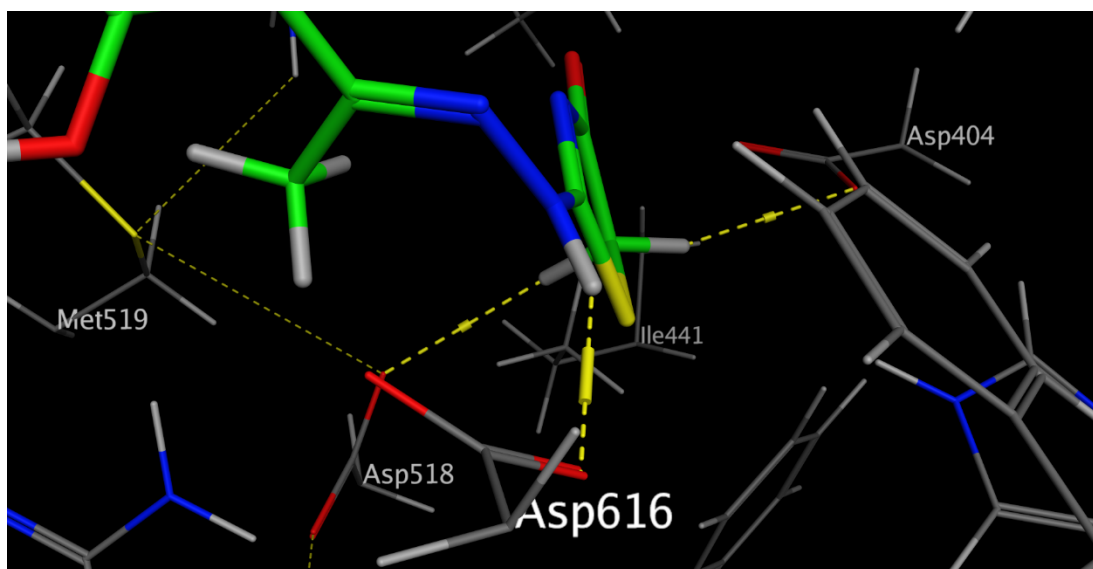
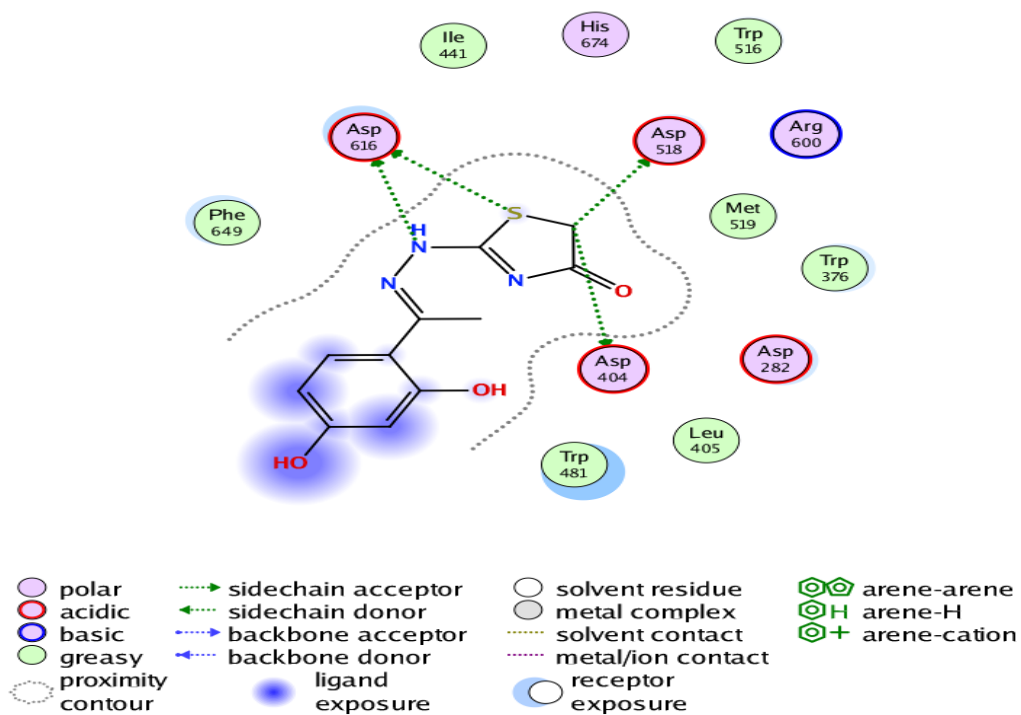


Figure 6: Component (3)'s 2D and 3D views inside the alpha-glucosidase receptor's active site.

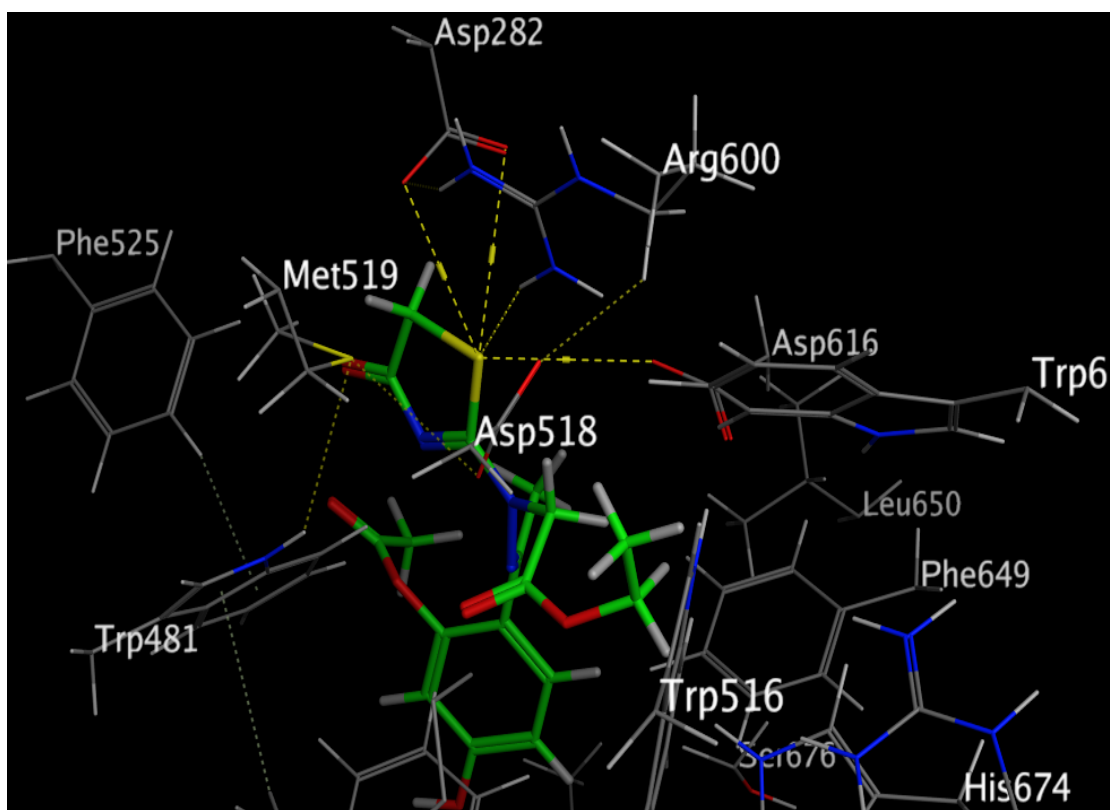
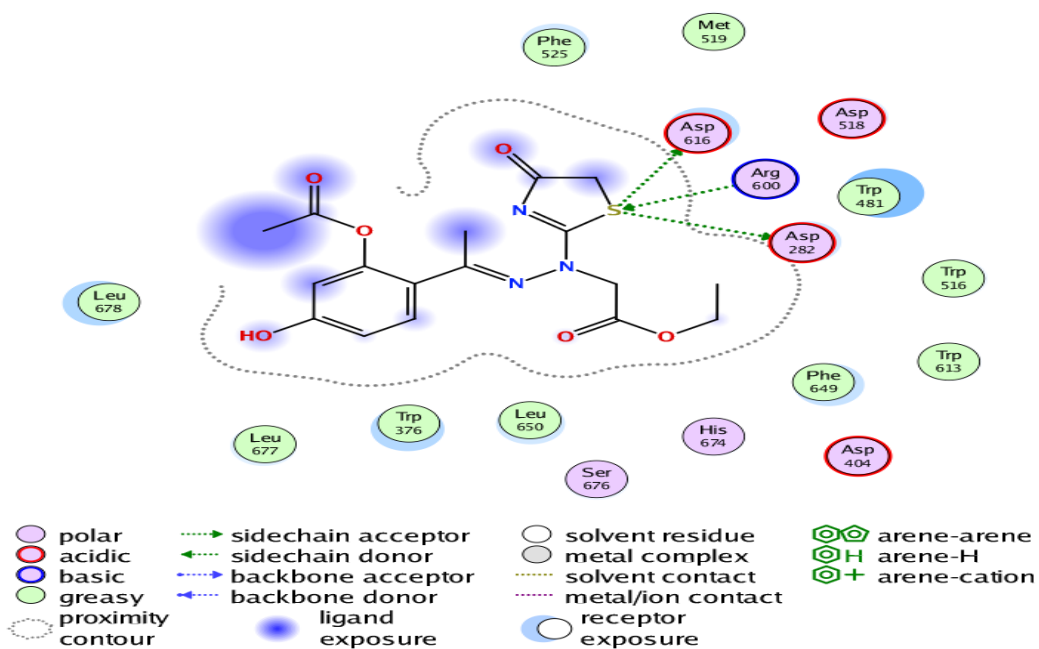


Figure 7: Component (7)'s 2D and 3D views inside the alpha-glucosidase receptor's active site.

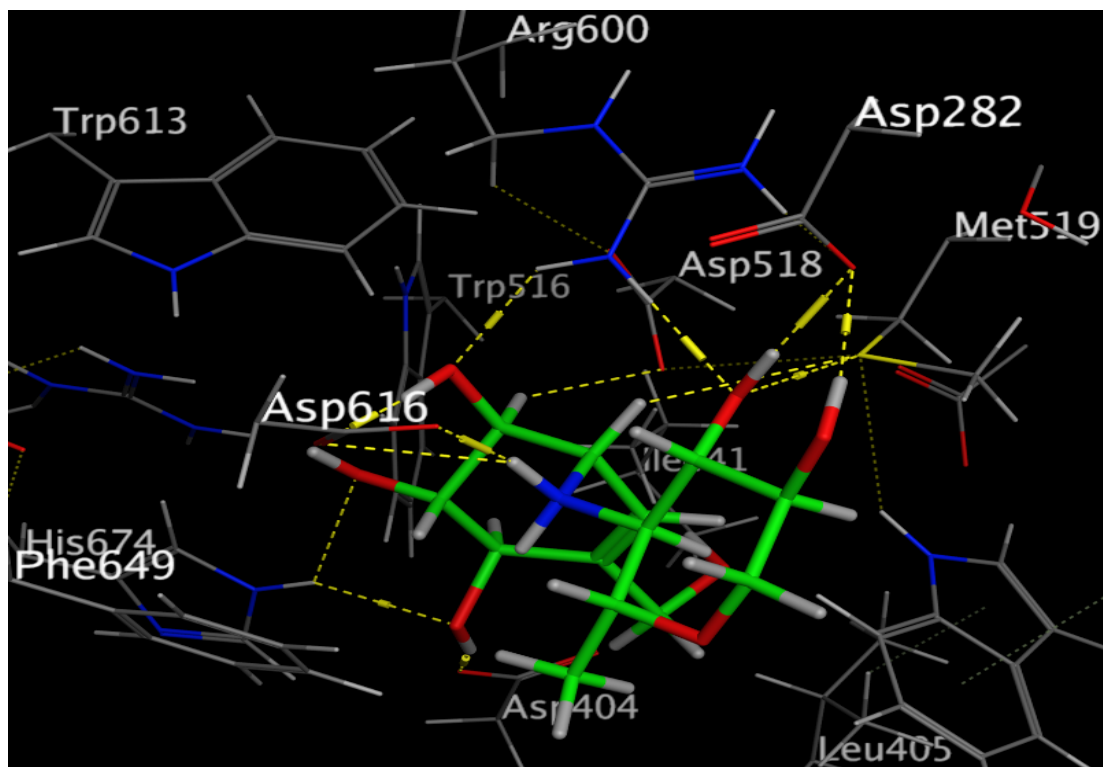
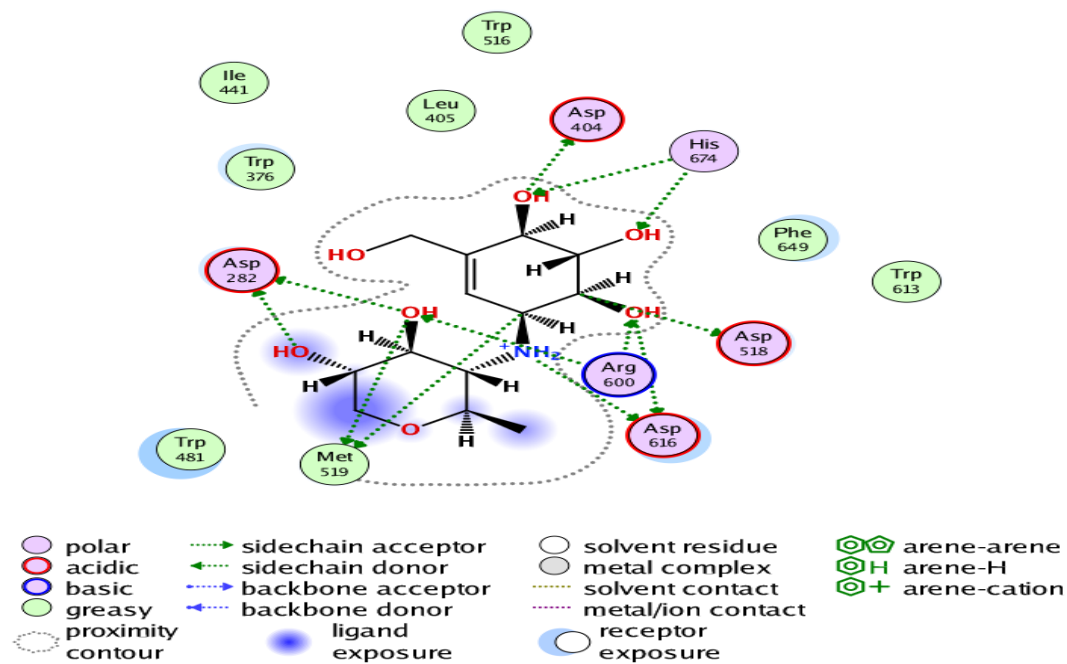


Figure 8: Views of acarbose at the α -glucosidase receptor's active site in 2D and 3D dimensions.

4. Conclusion

The present study was carried out for the synthesis of new hydrazinyl thiazole derivatives. Component (**5**) was synthesized through various synthetic protocol, and the majority of the components were gained in good yields. The approval of the proposed base of all the synthesized scaffolds was achieved with spectroscopic techniques. Biological screening of all synthesized components was carried out against α -glucosidase, glycation, and oxidation processes. The compound (**3**) showed an excellent α -glucosidase inhibitory action binding interaction of these compounds with α -glucosidase enzyme showed strong correlation with the experimental data. Inhibition of α -glucosidase enzyme, and compatible formation by these compounds suggest them as promising scaffolds for further studies.

Author contributions

The manuscript was written through contributions of all authors. All authors have given approval to the final version of the manuscript.

Conflict of Interest

The author declares no competing financial interest.

Acknowledgements

The author would like to acknowledge Deanship of Scientific Research, Taif University, for supporting this work.

References

- [1] T. Kalita, A. Choudhury, A. Shakya, A.K. Ghosh, U.p. Singh, H.R. Bhat, A Review on Synthetic Thiazole Derivatives as an Antimalarial Agent. *Current Drug Discovery Technologies*, 21(5) (2024) 10-42.
<https://doi.org/10.2174/0115701638276379231223101625>.
- [2] M.N. Bhoi, M.A. Borad, H.D. Patel, Synthetic strategies for fused benzothiazoles: past, present, and future. *Synthetic Communications*, 44(17) (2014) 2427-2457.
<https://doi.org/10.1080/00397911.2014.907426>.
- [3] D.S. Bhagat, P.A. Chawla, W.B. Gurnule, S.K. Shejul, G.S. Bumbrah, An insight into synthesis and anticancer potential of thiazole and 4-thiazolidinone containing motifs. *Current Organic Chemistry*, 25(7) (2021) 819-841.
<https://doi.org/10.2174/1385272825999210101234704>.
- [4] H.K. Thabet, Y.A. Ammar, M. Imran, M.H. Helal, S.I. Alaql, A. Alshehri, A. Ragab, Unveiling anti-diabetic potential of new thiazole-sulfonamide derivatives: Design, synthesis, in vitro bio-evaluation targeting DPP-4, α -glucosidase, and α -amylase with in-silico ADMET and docking simulation. *Bioorganic Chemistry*, 151 (2024) 107671.
<https://doi.org/10.1016/j.bioorg.2024.107671>.
- [5] M. Rashid *et al.*, Design and synthesis of benzimidazoles containing substituted oxadiazole, thiadiazole and triazolo-thiadiazines as a source of new anticancer agents, *Arabian Journal of Chemistry*, 12(8) (2019) 3202-3224.
<https://doi.org/10.1016/j.arabjc.2015.08.019>.
- [6] D. Havrylyuk, O. Roman, R. Lesyk, Synthetic approaches, structure activity relationship and biological applications for pharmacologically attractive pyrazole/pyrazoline-thiazolidine-based hybrids, *European journal of medicinal chemistry*, 113 (2016) 145-166.
<https://doi.org/10.1016/j.ejmech.2016.02.030>.
- [7] G. R. Ashour *et al.*, Synthesis, modeling, and biological studies of new thiazole-pyrazole analogues as anticancer agents, *Journal of Saudi Chemical Society*, (023) 101669.
<https://doi.org/10.1016/j.jscs.2023.101669>.
- [8] K. S. S. Kumar *et al.*, Antiproliferative and tumor inhibitory studies of 2, 3 disubstituted 4-thiazolidinone derivatives, *Bioorganic & medicinal chemistry letters*, 25(17) (2015) 3616-3620.
<https://doi.org/10.1016/j.bmcl.2015.06.069>.
- [9] P. C. Sharma *et al.*, Thiazole-containing compounds as therapeutic targets for cancer therapy, *European journal of medicinal chemistry*, 188 (2020) 112016.
<https://doi.org/10.1016/j.ejmech.2019.112016>.
- [10] T. Al-Warhi *et al.*, Novel 2-(5-Aryl-4, 5-dihydropyrazol-1-yl) thiazol-4-one as EGFR inhibitors: synthesis, biological assessment and molecular docking insights, *Drug Design, Development and Therapy*, (2022) 1457-1471.
<https://doi.org/10.2147/DDDT.S356988>.
- [11] A. Alsayari *et al.*, Synthesis, Characterization, and Biological Evaluation of Some Novel Pyrazolo [5, 1-b] thiazole Derivatives as Potential Antimicrobial and Anticancer Agents, *Molecules*, 26(17) (2021) 5383.
<https://doi.org/10.3390/molecules26175383>.
- [12] M. D. Altntop *et al.*, Design, Synthesis, and Evaluation of a New Series of Thiazole-Based Anticancer Agents as Potent Akt Inhibitors, *Molecules*, 23(6) (2018) 1318.
<https://doi.org/10.3390/molecules23061318>.
- [13] K. Liaras, M. Fesatidou, A. Geronikaki, Thiazoles and Thiazolidinones as COX/LOX Inhibitors, *Molecules*, 23(3) (2018) 685.
<https://doi.org/10.3390/molecules23030685>.
- [14] S.K. Manjal, R. Kaur, R. Bhatia, K. Kumar, V. Singh, R. Shankar, R.K. Rawal, Synthetic and medicinal perspective of thiazolidinones: A review. *Bioorganic Chemistry*, 75 (2017) 406-423.
<https://doi.org/10.1016/j.bioorg.2017.10.014>.

- [15] R. Bhutani, D.P. Pathak, G. Kapoor, A. Husain, M. A. Iqbal, Novel hybrids of benzothiazole-1, 3, 4-oxadiazole-4-thiazolidinone: Synthesis, in silico ADME study, molecular docking and in vivo anti-diabetic assessment. *Bioorganic chemistry*, 83 (2019) 6-19.
<https://doi.org/10.1016/j.bioorg.2018.10.025>.
- [16] S. Hameed, K.M. Khan, U. Salar, M., Özil, N. Baltaş, F. Saleem, Z. Ul-Haq, Hydrazinyl thiazole linked indenoquinoxaline hybrids: Potential leads to treat hyperglycemia and oxidative stress; Multistep synthesis, α -amylase, α -glucosidase inhibitory and antioxidant activities. *International Journal of Biological Macromolecules*, 221 (2022)1294-1312.
<https://doi.org/10.1016/j.ijbiomac.2022.09.102>.
- [17] M.A. Abid, A.A. Abed, M. Musa, T. Izuagie, E.C. Agwamba, Anti-Diabetic, Anti-Bacterial and Anti-Oxidant Potential of New Biologically Active Thiazole-Derivatives: Experimental and Molecular Docking Studies. *Journal of Molecular Structure*, 1321 (2024)139482.
<https://doi.org/10.1016/j.molstruc.2024.139482>.
- [18] M. Sawant, N. Chandan, Aromatic C-acylation of Phenols by using Acid and Acid Anhydride in Presence of Lewis Acid Catalyst, *Am. J. PharmTech Res.* 8(5) (2018).
- [19] S. Hameed, K.M. Khan, U. Salar, M. Özil, N. Baltaş, F. Saleem, Z. Ul-Haq, Hydrazinyl thiazole linked indenoquinoxaline hybrids: Potential leads to treat hyperglycemia and oxidative stress; Multistep synthesis, α -amylase, α -glucosidase inhibitory and antioxidant activities. *International Journal of Biological Macromolecules*, 221 (2022) 1294-1312.
<https://doi.org/10.1016/j.ijbiomac.2022.09.102>.
- [20] A.A. Mourad, N.A. Farouk, E.S.H. El-Sayed, A.R. Mahdy, EGFR/VEGFR-2 dual inhibitor and apoptotic inducer: Design, synthesis, anticancer activity and docking study of new 2-thioxoimidazolidin-4-one derivatives. *Life Sciences*, 277 (2021)119531.
<https://doi.org/10.1016/j.lfs.2021.119531>.
- [21] S.J. Yang, W.J. Lee, E.A. Kim, K. Dal Nam, H.G. Hahn, S.Y. Choi, S.W. Cho, Effects of N-adamantyl-4-methylthiazol-2-amine on hyperglycemia, hyperlipidemia and oxidative stress in streptozotocin-induced diabetic rats. *European journal of pharmacology*, 736 (2014) 26-34.
<https://doi.org/10.1016/j.ejphar.2014.04.031>.
- [22] A. Maslat, B. Al-Trad, I. Alameen, M. Al-Talib, H. Tashtoush, B. Ababneh, The Effect of Two Novel Substituted Thiazole and Thiadiazine Derivatives on Experimental Type-1 Diabetes Mellitus. *Jordan Journal of Chemistry*, 19(1) (2024) 41-47.
<https://jjc.yu.edu.jo/index.php/jjc/article/view/703>.
- [23] H. Mehmood, M. Haroon, T. Akhtar, S. Woodward, H. Andleeb, Synthesis and molecular docking studies of 5-acetyl-2-(arylidenehydrazin-1-yl)-4-methyl-1, 3-thiazoles as α -amylase inhibitors. *Journal of Molecular Structure*, 1250 (2022) 131807.
<https://doi.org/10.1016/j.molstruc.2021.131807>.
- [24] F.R. Santos, J.T. Andrade, C.D. Sousa, J.S. Fernandes, L.F. Carmo, M.G. Araújo, J.A. Villar, Synthesis and Evaluation of the in vitro Antimicrobial Activity of Triazoles, Morpholines and Thiosemicarbazones. *Medicinal Chemistry*, 15(1) (2019) 38-50.
<https://doi.org/10.2174/1573406414666180730111954>.
- [25] M.K. Kim, J.H. Suk, M.J. Kwon, H.S. Chung, C.S. Yoon, H.J. Jun, J.H. Ko, T.K. Kim, S.H. Lee, M.K. Oh, B.D. Rhee, J.H. Park, Nateglinide and acarbose for postprandial glucose control after optimizing fasting glucose with insulin glargine in patients with type 2 diabetes, *Diabetes Research and Clinical Practice* 92 (2011) 322–328.
<https://doi.org/10.1016/j.diabres.2011.01.022.22>.
- [26] M. Altay, Acarbose is again on the stage, *WJD* 13 (2022) 1–4. <https://doi.org/10.4239/wjd.v13.i1.1>.
- [27] M. Dvorakova, L. Langhansova, V. Temml, A. Pavicic, T. Vanek, P. Landa, Synthesis, Inhibitory Activity, and In Silico Modeling of Selective COX-1 Inhibitors with a Quinazoline Core, *ACS Med. Chem. Lett.* 12 (2021) 610–616. <https://doi.org/10.1021/acsmchemlett.1c00004>.
- [28] M. Sohrabi, M.R. Binaeizadeh, A. Iraj, B. Larijani, M. Saeedi, M. Mahdavi, A review on α -glucosidase inhibitory activity of first row transition metal complexes: a futuristic strategy for treatment of type 2 diabetes, *RSC Adv.* 12 (2022) 12011–12052. <https://doi.org/10.1039/d2ra00067a>.
- [29] S. Deng, A. Li, Y. Zhang, Discovery of the new alpha-glucosidase inhibitor with therapeutic potential in type 2 diabetes mellitus by a novel high-throughput virtual screening and free energy evaluation, *J. Mol. Graph. Model.* 121 (2023) 108447. <https://doi.org/https://doi.org/10.1016/j.jmgm.2023.108447>.
- [30] A.S. Alqahtani, S. Hidayathulla, M.T. Rehman, A.A. ElGamal, S. Al-Massarani, V. Razmovski-Naumovski, M.S. Alqahtani, R.A. El Dib, M.F. AlAjmi, Alpha-Amylase and Alpha-Glucosidase Enzyme Inhibition and Antioxidant Potential of 3-Oxolupenal and Katonic Acid Isolated from *Nuxia oppositifolia*, *Biomolecules*, 10 (2019).
<https://doi.org/10.3390/biom10010061>.
- [31] M. Telagari, K. Hullatti, In-vitro α -amylase and α -glucosidase inhibitory activity of *Adiantum caudatum* Linn and *Celosia argentea* Linn. extracts and fractions, *Indian J. Pharmacol.* 47 (2015) 425–429.
<https://doi.org/10.4103/0253-7613.161270>.
- [32] J. Feng, X.W. Yang, R.F. Wang, Bio-assay guided isolation and identification of α -glucosidase inhibitors from the leaves of *Aquilaria sinensis*, *Phytochemistry*, 72 (2011) 242–247.

- <https://doi.org/10.1016/j.phytochem.2010.11.025>.
- [33] C.F. Deacon, R.D. Carr, J.J. Holst, DPP-4 inhibitor therapy: new directions in the treatment of type 2 diabetes. *Front Biosci*, 13(5) (2008) 1780-1794.
<https://doi.org/10.2741/2799>.
- [34] S. Baliyan, R. Mukherjee, A. Priyadarshini, A. Vibhuti, A. Gupta, R.P. Pandey, C.M. Chang, Determination of Antioxidants by DPPH Radical Scavenging Activity and Quantitative Phytochemical Analysis of *Ficus religiosa*, *Molecules*, 27 (2022) 1326. <https://doi.org/10.3390/molecules27041326>.
- [35] V. Roig-Zamboni, B. Cobucci-Ponzano, R. Iacono, M.C. Ferrara, S. Germany, Y. Bourne, G. Parenti, M. Moracci, G. Sulzenbacher, Structure of human lysosomal acid α -glucosidase—a guide for the treatment of Pompe disease, *Nat. Commun.* 8 (2017) 1111. <https://doi.org/10.1038/s41467-017-01263-3>.
- [36] R. Thomsen, M.H. Christensen, MolDock: a new technique for high-accuracy molecular docking., *J. Med. Chem.* 49 (2006) 3315–3321.
<https://doi.org/10.1021/jm051197e>.
- [37] M. El Behery, I.M. El-Deen, M.A. El-Zend, L.A. Barakat, Design, synthesis and evaluation the bioactivities of novel 8-methoxy-1-azacoumarin-3-carboxamide derivatives as anti-diabetic agents. *Journal of Molecular Structure*, 1294 (2023) 136486.
<https://doi.org/10.1016/j.molstruc.2023.136486>.
- [38] I.M. El-Deen, M.A. El-Zend, M.A. Tantawy, L.A. Barakat, Synthesis and cytotoxicity screening of some synthesized coumarin and aza-coumarin derivatives as anticancer agents. *Russian Journal of Bioorganic Chemistry*, 48(2) (2022) 380-390.
DOI: 10.1134/S106816202202011X.
- [39] L.A. Ali Barakat, I.M. El-Deen, M.A. El-Zend, M. El-Behery, In vitro cytotoxic investigation of some synthesized 1, 6-disubstituted-1-azacoumarin derivatives as anticancer agents. *Future Medicinal Chemistry*, 15(24) (2023) 2289-2307.
<https://doi.org/10.4155/fmc-2023-0260>
- .